Synthesis, Crystal Structures and Thermal Properties of New ZnBr$_2$(pyrimidine) Coordination Compounds

Christian Näther,*[a] Gaurav Bhosekar,[a] and Inke Jeß[a]

Four new bromidozinc(II) coordination compounds with pyrimidine as a ligand were prepared, either in solution or by thermal decomposition reactions, and the thermal reactivity and thermodynamic stability of these compounds were investigated. These results are compared with those for the corresponding ZnI$_2$(pyrimidine) compounds. The ligand-rich 1:2 compound dibromidobis(pyrimidine-*N*)zinc(II) (**I**) crystallizes in the monoclinic space group *P*2$_1$/*n*. In this structure the zinc atoms are coordinated by two bromido ligands and two pyrimidine ligands within distorted tetrahedra. On heating, compound **I** is transformed into the ligand-deficient 2:3 intermediate bis(dibromido)bis(pyrimidine-*N*)(μ$_2$-pyrimidine-*N*,*N'*)dizinc(II) (**II**), which crystallizes in the monoclinic space group *C*2/*c*. The crystal structure consists of two ZnBr$_2$(pyrimidine) subunits, which are connected by an additional pyrimidine ligand through μ-*N*,*N'* coordination. Thermal decomposition of compound **II** leads to the formation of the ligand-deficient 1:1 compound dibromido(μ$_2$-pyrimidine-*N*,*N'*)zinc(II) (**III**), which crystallizes in the orthorhombic space group *Pmma*. In compound **III**, the zinc atoms are coordinated by four bromine atoms and two pyrimidine ligands within distorted octahedra. The ZnBr$_2$ units are connected through common edges into chains, which are linked by the pyrimidine ligands into layers. On heating, compound **III** is transformed into the ligand-deficient 2:1 compound (ZnBr$_2$)$_2$-(pyrimidine) (**IV**), which decomposes to give ZnBr$_2$. Solvent-mediated conversion experiments in solution show that not all of the compounds can be prepared by treating ZnBr$_2$ and pyrimidine in the molar ratio given by the formula of the final product.

(© Wiley-VCH Verlag GmbH & Co. KGaA, 69451 Weinheim, Germany, 2007)

Introduction

Investigations on coordination polymers, inorganic–organic hybrid compounds and metal–organic frameworks are attracting increasing interest[1] because of the potential applications of these systems as electric, magnetic, optical or porous materials.[2] Most of these compounds are normally prepared in solution, where different stable and metastable species exist in equilibrium. In view of this, mixtures of compounds are often obtained during the synthesis, and some specific target compounds cannot be prepared at all. Recently we have demonstrated that thermal decomposition of ligand-rich precursor materials is a suitable alternative method for the convenient synthesis of new coordination compounds.[3] In this method, ligand-rich precursors are heated, leading to ligand-deficient coordination compounds by stepwise liberation of the ligands. One advantage of this method is that the equilibrium is shifted irreversibly in the direction of the ligand-deficient coordination compounds, and thus new compounds which are metastable or unstable in solution can be discovered and prepared as phase-pure solids.

Recently we have reported on new iodidozinc(II) coordination compounds with pyrimidine as a ligand.[4] Altogether, seven different compounds were obtained, including three polymorphic modifications (Figure 1). The ligand-rich 1:2 compound **1** decomposes in several steps, in which ligand-deficient compounds **2**, **3** and **4** [2:3 (**2**), 1:1 (**3**) and 2:1 (**4**)] are formed as intermediates. Detailed analysis of the crystal structures of these compounds clearly indicates a strong correlation between the crystal structures of the reactants and the products for the first two thermal reactions. Slight changes in the reaction conditions lead to the formation of a further 1:1 compound of composition [ZnI$_2$(pyrimidine)]$_4$(acetonitrile)$_{0.25}$ (**5**). On heating, compound **5** loses acetonitrile and decomposes to give a new 1:1 polymorphic modification **6**. Compound **6** undergoes a polymorphic phase transition to yield the new compound **7**, which is finally transformed into the 1:1 compound **3**. Solvent-mediated conversion experiments clearly show that compound **3** represents the thermodynamically most stable form at room temperature, whereas **5**, **6** and **7** are metastable. Our results clearly show that different stable and metastable species are in equilibrium and that product formation in such thermal decomposition reactions depends on the actual structure of the ligand-rich precursor compound.

[a] Institut für Anorganische Chemie, Universität zu Kiel,
Olshausenstr. 40 (Otto-Hahn-Platz 6–7), 24098 Kiel
Fax: +49-431-880-1520
E-mail: cnaether@ac.uni-kiel.de
Supporting information for this article is available on the WWW under http://www.eurjic.org or from the author.
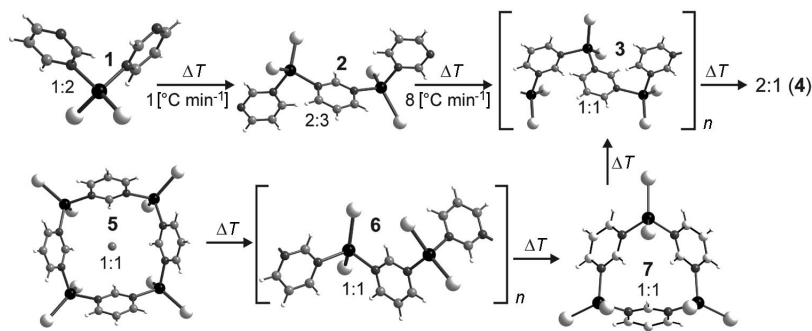
C. Näther, G. Bhosekar, I. Jeß

Figure 1. Schematic presentation of the thermal reactions of ZnI_2(pyrimidine) coordination compounds.[4]

In order to gain more insight into such reactions, we have investigated the corresponding compounds with $ZnBr_2$ and pyrimidine. Here we report on the results of these investigations.

Results and Discussion

Crystal Structures

The ligand-rich 1:2 compound **I** crystallizes in the monoclinic space group $P2_1/n$ with four formula units in the unit cell and all atoms in general positions. The crystal structure of **I** is isomorphous to ZnI_2(pyrimidine)$_2$.[4] In the crystal structure, there are discrete complexes, in which the zinc atoms are coordinated by two bromine atoms and two nitrogen atoms of the pyrimidine ligands within distorted tetrahedra (Figure 2: top and Table 1). The pyrimidine ligands of adjacent complexes are stacked in the direction of the crystallographic *a* axis, which indicates π–π interactions (Figure 2: bottom).

The ligand-deficient 2:3 intermediate **II** crystallizes in the monoclinic space group $C2/c$ with eight formula units in the unit cell. This compound is isomorphous to $(ZnI_2)_2$-(pyrimidine)$_3$.[4] In the crystal structure discrete [(ZnBr$_2$)$_2$-(pyrimidine)$_3$] units are found, which are located in special positions (Figure 3: top). Each zinc atom is coordinated by two bromine atoms and two nitrogen atoms, one on a terminal and one on a bridging pyrimidine ligand (Figure 3: top and Table 1). The zinc atoms are bridged by a pyrimidine ligand with μ-N,N' coordination. The terminal pyrimidine rings are stacked in the direction of the crystallographic *b* axis, indicating π–π interactions (Figure 3: bottom).

The ligand-deficient 1:1 compound **III** crystallizes in the orthorhombic space group *Pmma* with two formula units in the unit cell. The zinc and the bromine atoms as well as the pyrimidine ligands are located on crystallographic mirror planes. This compound is not isomorphous to the corresponding iodido analogue ZnI_2(pyrimidine).[4] In this structure the zinc atoms are coordinated by four bromine atoms and two nitrogen atoms of pyrimidine ligands within slightly distorted octahedra (Figure 4: top and Table 1). The zinc atoms are connected by the pyrimidine ligands into zigzag chains, which elongate in the direction of the crystallo-
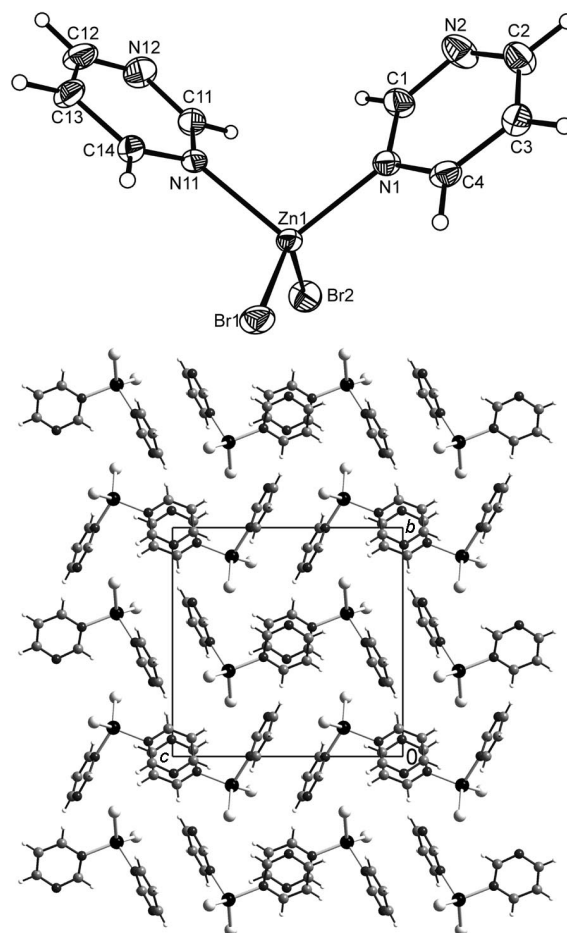

Figure 2. Crystal structure of compound **I** with a view of the coordination sphere of the zinc cations with labelling and displacement ellipsoids drawn at the 50% probability level (top) and a view of the crystal structure in the direction of the crystallographic *a* axis (bottom).

graphic *a* axis (Figure 4: middle). The zinc octahedra are additionally connected through common Br edges into corrugated layers, which are located in the *ab* plane (Figure 4: bottom).

Table 1. Bond lengths [Å] and angles [°] for compounds **I**, **II** and **III**.[a]

Compound **I**			
Zn1–N1	2.063(3)	Zn1–N11	2.081(3)
Zn1–Br2	2.3489(6)	Zn1–Br1	2.3500(5)
N1–Zn1–Br2	110.55(9)	N11–Zn1–Br2	105.50(9)
N1–Zn1–Br1	106.94(9)	N1–Zn1–N11	102.79(11)
Br2–Zn1–Br1	124.12(2)	N11–Zn1–Br1	104.78(8)
Compound **II**			
Zn1–N11	2.070(4)	Zn1–Br2	2.3333(8)
Zn1–N1	2.091(4)	Zn1–Br1	2.3523(8)
N11–Zn1–N1	101.21(16)	N11–Zn1–Br1	104.80(12)
N11–Zn1–Br2	110.28(13)	N1–Zn1–Br1	105.97(11)
N1–Zn1–Br2	110.37(11)	Br2–Zn1–Br1	122.10(3)
Compound **III**			
Zn1–N1	2.178(3)	Zn1–Br1	2.6287(3)
Zn1–N1B	2.178(3)	Zn1–Br1D	2.6287(3)
Zn1–Br1B	2.6287(3)	Zn1–Br1C	2.6287(3)
Br1–Zn1E	2.6287(3)	Br1–Zn1–Br1D	89.056(12)
N1–Zn1–N1B	180.00(17)	N1–Zn1–Br1C	89.93(6)
N1–Zn1–Br1B	90.07(6)	N1B–Zn1–Br1C	90.07(6)
N1B–Zn1–Br1B	89.93(6)	Br1B–Zn1–Br1C	89.056(12)
N1–Zn1–Br1	89.93(6)	Br1–Zn1–Br1C	90.944(12)
N1B–Zn1–Br1	90.07(6)	Br1D–Zn1–Br1C	180.0
Br1B–Zn1–Br1	180.0	C1–N1–Zn1	122.3(3)
N1–Zn1–Br1D	90.07(6)	C2–N1–Zn1	120.8(3)
N1B–Zn1–Br1D	89.93(6)	Br1B–Zn1–Br1D	90.944(12)

[a] Symmetry transformations used to generate equivalent atoms: A: −x + 3/2, −y, z; B: −x + 1, −y, −z; C: x, y − 1, z; D: −x + 1, −y + 1, −z.
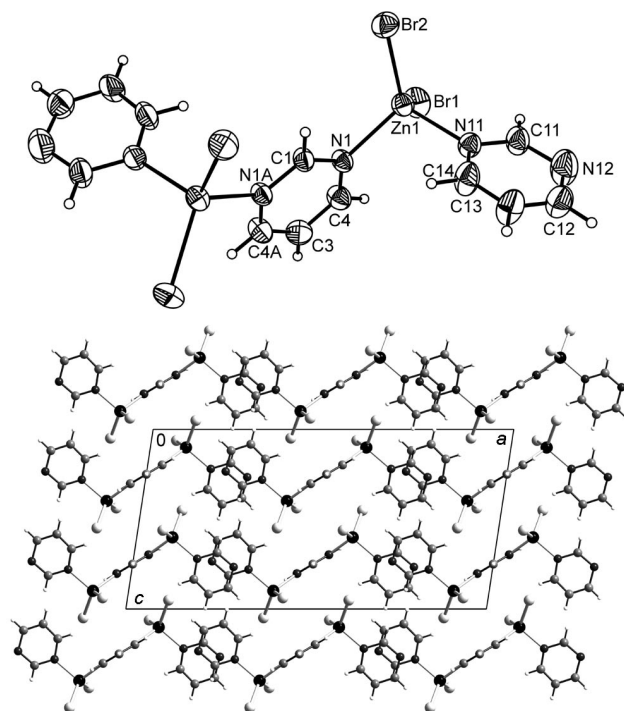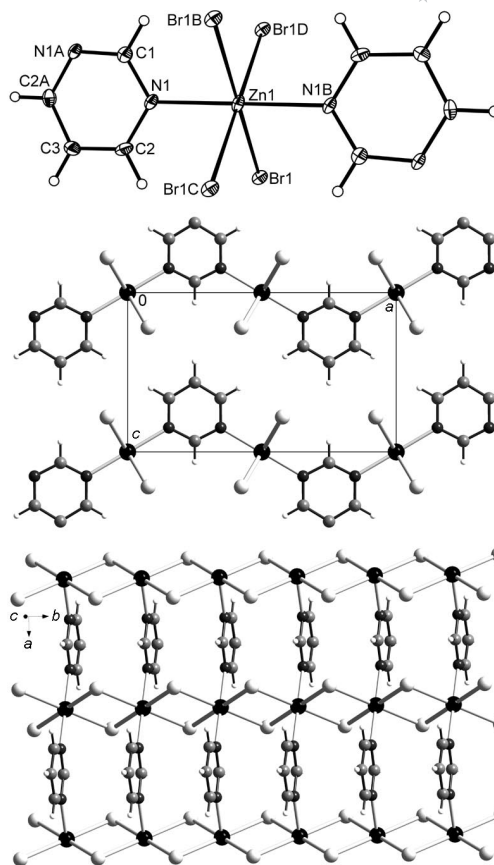

Figure 4. Crystal structure of compound **III** with a view of the coordination sphere of the zinc cations with labelling and displacement ellipsoids drawn at the 50% probability level (top; symmetry codes: A: −x + 1, −y, −z; B: x, y − 1, z; C: −x + 1, −y + 1, −z) and a view of the structure in the direction of the crystallographic *b* axis (bottom).

Figure 3. Crystal structure of compound **II** with a view of the coordination sphere of the zinc cations with labelling and displacement ellipsoids drawn at the 50% probability level (top; symmetry codes: A = −x, y, −z + 3/2) and a view of the crystal structure in the direction of the crystallographic *b* axis (bottom).

Thermoanalytical Investigations

Five mass steps are observed for compound **1** on heating, of which the first four steps are accompanied by endothermic events in the DTA curve (Figure 5). From the MS trend scan curve it is evident that only pyrimidine ligands ($m/z = 80$) are liberated in the first four steps and the DTG curve shows that not all of the steps are well resolved. The experimental mass loss in each of the first four TG steps is in good agreement with that calculated for the removal of half of the pyrimidine ligands in each step (Δm_{theo} −1/2 pyrimidine = −10.4%) (Figure 5). Thus, it can be inferred that in these steps a ligand-deficient 2:3, 1:1 and 2:1 compound is formed, which finally decomposes to give $ZnBr_2$, which vaporizes on further heating.

In order to determine the nature of the thermal decomposition products, additional thermogravimetric measurements were performed in which the heating was stopped after each step. The residues thus obtained were investigated by X-ray powder diffraction (Figure 6) and elemental analysis; the results are presented in the Experimental Section.
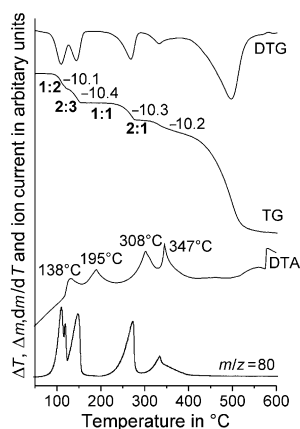
Figure 5. DTA, TG, DTG and MS trend scan curves for compound **I** [heating rate: 4 °C min⁻¹; m/z = 80 (pyrimidine)]; given are the mass changes [%] and the peak temperatures T_p [°C].
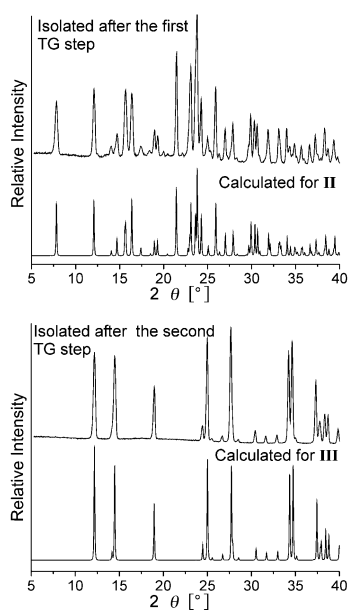

Figure 6. Experimental X-ray powder diffraction pattern of the residue obtained after the first (top) and second (bottom) TG step in the thermal decomposition of the ligand-rich 1:2 compound **I**, accompanied by the calculated X-ray powder diffraction patterns for compounds **II** and **III**.

The experimental X-ray powder diffraction patterns of the residues formed in the first and second TG steps are in excellent agreement with those calculated for compounds **II** and **III**, clearly indicating that in the first TG step the ligand-deficient 2:3 intermediate **II** is formed, and then it is transformed into the ligand-deficient 1:1 compound **III** on further heating (Figure 5 and Figure 6). In addition, the results of an elemental analysis of the residues agrees with the expected results for a 2:3 and 1:1 compound (Experimental Section). These results show that both compounds are obtained as phase-pure solids even though the first TG step is not well resolved. It is interesting to note that the powder pattern of the residue formed in the third step matches well

with that of the pattern of a solid obtained by stirring a crystalline suspension of $ZnBr_2$ and pyrimidine in *n*-hexane for several days. This result indicates that the ligand-deficient compound **IV** can also be prepared in solution.

The elemental analysis of the residue formed in the third TG step corresponds to a new compound of 2:1 stoichiometry of composition $(ZnBr_2)_2$(pyrimidine) (**IV**). As expected, the experimental X-ray powder diffraction pattern of this compound is completely different from that calculated for compounds **II** and **III** and for $ZnBr_2$ (Figure 7).
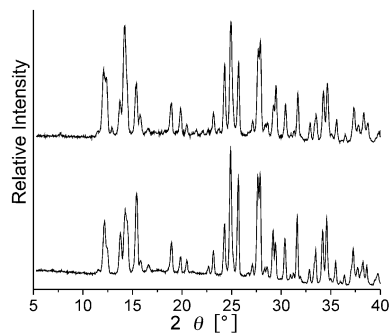

Figure 7. Experimental X-ray powder diffraction pattern of the residue obtained after the third TG step during the thermal decomposition of the ligand-rich 1:2 compound **I** (top) and the experimental X-ray powder diffraction pattern for compound **IV** obtained from solution (bottom).

Investigations on the Stability of the Compounds in Solution and in the Solid State

The stability of compounds **I**, **II** and **III** as solids was investigated by time-dependent X-ray powder diffraction. These investigations show that compounds **II** and **III** are stable over several days, whereas the ligand-rich 1:2 compound **I** decomposes even at room temperature within a few days to give compound **III**.

The stability of these compounds was further investigated in solution by solvent-mediated conversion experiments. In these experiments the metal salt and ligand are mixed in different stoichiometric ratios by using acetonitrile as a solvent. These crystalline suspensions were stirred for a week in order to obtain the thermodynamically most stable form. Afterwards the products were investigated by X-ray powder diffraction (Table 2). These experiments clearly showed that all compounds are stable and can also be prepared in solution. However, it is to be noted that not all of these compounds can be prepared simply by mixing the reactants stoichiometrically as given by the formula. Thus, the reaction of $ZnBr_2$ and pyrimidine in 2:3 mol ratio results in the formation of the 1:1 compound **III**, whereas

Table 2. Result of the crystallization experiments in different solvents as a function of the molar ratio between metal and ligand (pyrimidine).

ZnBr₂/Ligand	1:4	1:3	1:2	2:3	1:1	2:1
Compound	**I** (1:2)		**II** (2:3)	**III** (1:1)		**IV**(2:1)

the reaction in a 1:2 mol ratio leads to the formation of the 2:3 compound **II** (Table 2). This indicates that for the preparation of the ligand-rich compounds, an excess of the ligand must always be used. The ligand-deficient compound **IV** is difficult to prepare, because in many cases it is contaminated with compound **III** or $ZnBr_2$ (Table 2).

Comparison of ZnX_2(pyrimidine) Coordination Compounds (X = Cl, I)

As mentioned earlier, for the corresponding coordination compounds with ZnI_2 a variety of compounds and polymorphic modifications were found.[4] The different polymorphic modifications were detected when the pseudopolymorphic 1:1 compound $[ZnI_2$(pyrimidine)]$_4$(acetonitrile)$_{0.25}$ was decomposed, which was prepared by fast precipitation under kinetic control from a solution of ZnI_2 and pyrimidine in acetonitrile by adding an antisolvent in which the compound is insoluble. In view of this observation, several attempts were made to prepare the corresponding acetonitrile solvate of the bromide compound. However, this always resulted in the formation of the ligand-deficient 1:1 compound **III**. From ZnI_2 and pyrimidine, two metastable polymorphic modifications of the 1:1 compound could also be prepared by performing the crystallization under kinetic control.[4] Similar attempts to prepare such forms of the bromide compound by nucleation-controlled crystallization[5] did not result in any polymorphic modifications. It must also be noted that the reaction of $ZnCl_2$ with pyrimidine leads only to one compound of composition $ZnCl_2$(pyrimidine),[6] which shows that the number of possible compounds in the ZnX_2(pyrimidine) [X = I, Br, Cl] system decreases from iodine to chlorine.

Differences between the ZnI_2 and $ZnBr_2$ coordination compounds are also found in the thermal reactivity of the ligand-rich 1:2 compounds, which are isotypic. On slow heating ZnI_2(pyrimidine)$_2$ (**1**) is transformed directly into the ligand-deficient 1:1 compound ZnI_2(pyrimidine) (**3**), without the formation of the ligand-deficient 2:3 intermediate **2**. Compound **2** can only be obtained by thermal decomposition if fast heating rates are used, which shows that kinetics plays an important role in product formation. In contrast, thermal decomposition of $ZnBr_2$(pyrimidine)$_2$ (**I**)

leads directly to the formation of the 2:3 compound $(ZnBr_2)_2$-(pyrimidine)$_3$, regardless of the actual heating rate.

In this context, it must be mentioned that for the decomposition reaction of the discrete units in ZnI_2(pyrimidine)$_2$ (**1**), via the oligomeric units in $(ZnI_2)_2$(pyrimidine)$_3$ (**2**), to the chains in ZnI_2(pyrimidine) (**3**), a smooth reaction pathway can be found (Figure 8: left).[4] In contrast, only for the reaction of $ZnBr_2$(pyrimidine)$_2$ (**I**) to give $(ZnBr_2)_2$(pyrimidine)$_3$ (**II**) a smooth reaction pathway is found, whereas for the transformation of the 2:3 intermediate **II** into the ligand-deficient 1:1 compound **III**, large translational and rotational changes are needed and thus no smooth reaction pathway can be expected (Figure 8: right).

Conclusions

In this contribution we have presented four new coordination compounds based on $ZnBr_2$ and pyrimidine, which can be prepared by thermal decomposition from the ligand-rich compound $ZnBr_2$(pyrimidine). These compounds can also be prepared in solution; however, the ligand-rich compounds are only accessible if an excess of ligand is used. The reaction of $ZnBr_2$ and pyrimidine in a ratio given by the formula of the final compound does not lead to compounds **I** and **II**. This phenomenon is frequently observed in the preparation of such compounds, and therefore new compounds can be easily overlooked if the synthesis is performed only in solution. In contrast, by thermal decomposition of the ligand-rich compounds, all ligand-deficient compounds can be detected in a single measurement. A comparison of the thermal properties of these bromido complexes with those of the corresponding iodidozinc(II) and chloridozinc(II) coordination compounds reveals several differences, which include the influence of the actual heating rate on product formation, the mechanism of such reactions and the possibility of the preparation of thermodynamically metastable compounds and different polymorphic modifications.

Experimental Section

Synthesis of Compound I: $ZnBr_2$ (112.59 mg, 0.5 mmol) and pyrimidine (240.24 mg, 3.0 mmol) were mixed in acetonitrile (0.5 mL).
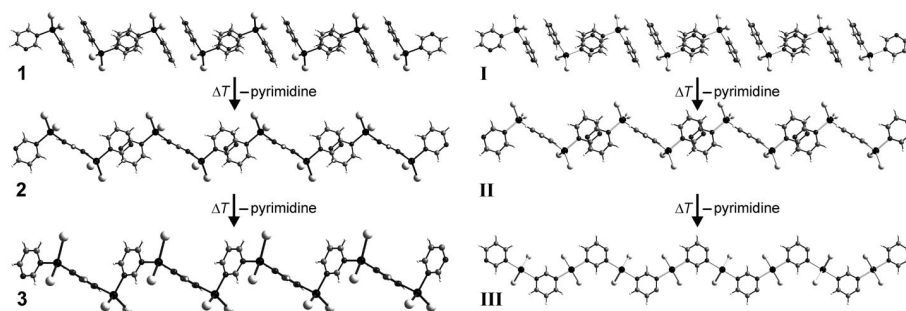

Figure 8. Structural relationships between the crystal structures of the ZnI_2(pyrimidine) (left) and $ZnBr_2$(pyrimidine) coordination polymers.

Afterwards, diethyl ether (1.0 mL) was added to the clear solution for precipitation. Yield: 133.6 mg (69.36%) based on ZnBr$_2$. C$_8$H$_8$Br$_2$N$_4$Zn (385.37): calcd. C 24.93, H 2.09, N 14.54; found C 25.02, H 2.18, N 14.63. IR (KBr): ṽ = 1591 (s), 1561 (m), 1471 (m), 1406 (s), 1369 (w), 1237 (w), 1174 (m), 1082 (m), 1016 (m), 817 (w), 705 (m), 688 (m), 643 (m) cm^{-1}. Single crystals were prepared by the reaction of ZnBr$_2$ (56.29 mg, 0.25 mmol) and pyrimidine (120.12 mg, 1.5 mmol) in acetonitrile (0.5 mL). Slow evaporation of the solvent from the clear solution yields colourless crystals in about a week.

Synthesis of Compound II: ZnBr$_2$ (112.59 mg, 0.5 mmol) and pyrimidine (80.08 mg, 1.0 mmol) were mixed in acetonitrile (0.5 mL). Afterwards, diethyl ether (1.0 mL) was added to the clear solution for precipitation. Yield: 161.9 mg (93.77%) based on ZnBr$_2$. C$_{12}$H$_{12}$Br$_4$N$_6$Zn$_2$ (690.66): calcd. C 20.87, H 1.75, N 12.17; found C 21.00, H 1.72, N 12.14. IR (KBr): ṽ = 3121 (w), 3095 (w), 3064 (m), 1594 (s), 1560 (s), 1472 (s), 1409 (s), 1228 (w), 1173 (m), 1081 (s), 1017 (m), 814 (m), 705 (s), 644 (m) cm^{-1}. Single crystals were prepared by the reaction of ZnBr$_2$ (112.59 mg, 0.5 mmol) and pyrimidine (80.08 mg, 1.0 mmol) in a mixture of acetonitrile (2.0 mL) and water (0.3 mL). Slow evaporation of the solvent yielded colourless crystals in about 4 d.

Synthesis of Compound III: ZnBr$_2$ (112.59 mg, 0.5 mmol) and pyrimidine (40.04 mg, 0.5 mmol) were mixed in acetonitrile (0.5 mL). Afterwards diethyl ether (1.0 mL) was added for precipitation. Yield: 129.3 mg (84.71%). C$_4$H$_4$Br$_2$N$_2$Zn (305.28): calcd. C 15.74, H 1.32, N 9.18; found C 15.87, H 1.29, N 9.09. IR (KBr): ṽ = 3121 (w), 3075 (w), 1595 (s), 1569 (m), 1465 (s), 1402 (s), 1356 (w), 1220 (m), 1180 (m), 1145 (w), 1081 (s), 1028(m), 933 (w), 801 (m), 688 (s), 661(s) cm^{-1}. Single crystals were prepared by the reaction of ZnBr$_2$ (22.51 mg, 0.1 mmol) and pyrimidine (8.08 mg, 0.1 mmol) in water (0.3 mL). Slow evaporation of the solvent yielded colourless crystals in about one week.

Synthesis of Compound IV: This compound was difficult to obtain in solution, because in most cases it was contaminated with compound **III**. From several reactions with different stoichiometric ratios of ZnBr$_2$ and pyrimidine, we obtained only one batch which was phase-pure. Its X-ray powder diffraction pattern is shown in Figure 7. However, the pure compound can be prepared in quanti-

tative yield by thermal decomposition of compound **I**, **II** or **III**. C$_4$H$_4$Br$_4$N$_2$Zn$_2$ (530.46): calcd. C 9.06, H 0.76, N 5.28; found C 9.13, H 0.81, N 5.35. IR (KBr): ṽ = 3106 (w), 3082 (w), 1684 (w), 1596 (s), 1569 (m), 1465 (s), 1403 (s), 1220 (m), 1180 (s), 1082 (s), 1028 (s), 801 (m), 689 (s), 660 (s) cm^{-1}.

Elemental Analysis of the Residues Obtained in the Thermal Decomposition of Compound I

(A) Isolated after the first heating step (compound **II**) C$_{12}$H$_{12}$Br$_4$N$_6$Zn$_2$ (690.66): calcd. C 20.87, H 1.75, N 12.17; found C 20.94, H 1.69, N 12.20. (B) Isolated after the second heating step (compound **III**) C$_4$H$_4$N$_2$Br$_2$Zn (305.28): calcd. C 15.74, H 1.32, N 9.18; found C 15.86, H 1.28, N 9.08. (C) Isolated after the third heating step (compound **IV**) C$_4$H$_4$Br$_4$N$_2$Zn$_2$ (530.46): calcd. C 9.06, H 0.76, N 5.28; found C 8.48, H 1.47, N 4.98.

Single Crystal Structure Analysis: All investigations were performed with an Imaging Plate Diffraction System (IPDS-1) from STOE & CIE. Structure solutions were performed with direct methods by using SHELXS-97,[7] and structure refinements were performed against F^2 with SHELXL-97.[7] For all structures a numerical absorption correction was applied by using X-Red[8] and X-Shape.[8] All non-hydrogen atoms were refined with anisotropic displacement parameters. All hydrogen atoms were positioned with idealized geometry and were refined with fixed isotropic displacement parameters [U_{eq}(H) = 1.2·U_{eq}(C)] by using a riding model with d_{C-H} = 0.95 Å. Details of the structural determination are given in Table 3 and in the Supporting Information.

CCDC-651854 (**I**), -651855 (**II**) and -651856 (**III**) contain the supplementary crystallographic data for this paper. These data can be obtained free of charge from The Cambridge Crystallographic Data Centre via www.ccdc.cam.ac.uk/data_request/cif.

X-ray Powder Diffraction: X-ray powder diffraction experiments were performed by using a STOE STADI P transmission powder diffractometer with Cu-K_α-radiation (λ = 154.0598 pm), which is equipped with a position-sensitive detector (scan range: 5°–45°) from STOE & CIE.

Differential Thermal Analysis, Thermogravimetry and Mass Spectrometry: The heating-rate-dependent DTA-TG measurements were performed under a nitrogen atmosphere (purity: 5.0) with

Table 3. Crystal data and results of the structural refinement for compounds **I**, **II** and **III**.

Compound	I	II	III
Chemical formula	C$_8$H$_8$Br$_2$N$_4$Zn	C$_{12}$H$_{12}$Br$_4$N$_6$Zn$_2$	C$_4$H$_4$N$_2$Br$_2$Zn
Formula weight	385.37	690.66	305.28
Crystal system	monoclinic	monoclinic	orthorhombic
Space group	$P2_1/n$	$C2/c$	$Pmma$
a [Å]	7.6087(6)	22.8319(19)	12.2327(14)
b [Å]	12.4580(8)	7.7361(5)	3.7481(3)
c [Å]	12.5606(10)	11.4845(9)	7.2659(6)
β [°]	91.854 (10)°	98.656(10)	–
Volume [Å^3]	1189.99 (15)	2005.4(3)	333.14(5)
Z	4	8	2
Calculated density [gcm^{-3}]	2.151	2.288	3.043
μ [mm^{-1}]	8.751	10.369	15.578
2θ range [°]	2.30 to 28.03	2.78 to 28.03	2.80 to 28.04
Measured reflections	11267	9201	3127
Unique reflections	2778	2394	478
Observed reflections [$I>2\sigma(I)$]	2341	1809	441
R_1[a] [$I>2\sigma(I)$]	0.0360	0.0413	0.0268
wR_2[b] [all data]	0.0968	0.1168	0.0697
GOF	1.026	1.024	1.100
Residual electron density [eÅ^{-3}]	0.778/–0.918	0.908/–0.759	1.106/–1.128

[a] $R_1 = \Sigma \,||F_o| - |F_c||/\Sigma|F_o|$. [b] $wR_2 = \{\Sigma[w(F_o{}^2 - F_c{}^2)^2]/\Sigma[w(F_o{}^2)^2]\}^{1/2}$.

Al$_2$O$_3$ crucibles in a STA-409CD instrument from Netzsch. The DTA-TG-MS measurements were performed with the same instrument, which is connected to a quadrupole mass spectrometer from Balzers by a Skimmer coupling from Netzsch. The MS measurements were performed in analog and trend scan mode in Al$_2$O$_3$ crucibles in a dynamic nitrogen atmosphere (purity: 5.0) by using heating rates of 4 °C min^{-1}. All measurements were performed with a flow rate of 75 mL min^{-1} and were corrected for buoyancy and current effects. The instrument was calibrated by using standard reference materials.

Elemental Analysis: CHN analysis has been performed with a EURO EA Elemental Analyzer, fabricated by EURO VECTOR Instruments and Software.

Supporting Information (see footnote on the first page of this article): Tables with bond lengths and angles and details of the structure determinations. Experimental and calculated X-ray powder diffraction patterns for compounds **I**–**III**. IR and Raman spectra of compounds **I**–**III**.

Acknowledgments

[1] a) A. Y. Robin, K. M. Fromm, *Coord. Chem. Rev.* **2006**, *250*, 2127–2157; b) P. J. Hagrman, D. Hagrman, J. Zubieta, *Angew. Chem. Int. Ed.* **1999**, *38*, 2638–2684; c) S. L. James, *Chem. Soc. Rev.* **2003**, *5*, 276–288; d) R. Robson in *Comprehensive Supramolecular Chemistry*, Pergamon, New York, **1996**, ch. 22, p. 733; e) R. Robson, B. F. Abrahams, S. R. Batten, R. W. Grable, B. F. Hoskins, J. Liu in *Supramolecular Architecture*, ACS publications, Washington DC, **1992**, ch. 19; f) S. R. Batten, R. Robson, *Angew. Chem.* **1998**, *110*, 1558–1595; *Angew. Chem. Int. Ed. Engl.* **1998**, *37*, 1460–1494; g) P. J. Hagrman, D. Hagrman, J. Zubieta, *Angew. Chem.* **1999**, *111*, 2798–2848; *Angew. Chem. Int. Ed.* **1999**, *38*, 2638–2684; h) A. J. Blake, N. R. Champness, P. Hubberstey, W.-S. Li, M. A. Withersby, M. Schröder, *Coord. Chem. Rev.* **1999**, *183*, 117–138; i) D. Braga, L. Maini, M. Polito, L. Scaccianoce, G. Cojazzi, F. Grepioni, *Coord. Chem. Rev.* **2001**, *216*–217; j) M. Kosal, J. Chou, S. Wilson, K. Suslick, *Nat. Mater.* **2002**, *1*, 118–121; k) O. M. Yaghi, H. Li, C. Davis, D. Richardson, T. L. Groy, *Acc. Chem. Res.* **1998**, *31*, 474–484.

[2] a) S. Kitagawa, K. Uemura, *Chem. Soc. Rev.* **2005**, *34*, 109–119; b) P. Horcajada, C. Serre, M. Vallet-Regi, M. Sebban, F. Taulelle, G. Ferey, *Angew. Chem. Int. Ed.* **2006**, *45*, 5974–5978; c) B. Paul, C. Näther, B. Walfort, K. M. Fromm, B. Zimmermann, H. Lang, C. Janiak, *Cryst. Eng. Commun.* **2005**, *7*, 309–319; d) M. Eddaoudi, J. Kim, N. Rosi, D. Vodak, J. Wachter, M. O'Keefe, O. M. Yaghi, *Science* **2002**, *295*, 469–472; e) J. L. C. Rowsell, O. M. Yaghi, *Microporous Mesoporous Mater.* **2004**, *73*, 3–14; f) H. K. Chae, D. Y. Siberio-Perez, J. Kim, Y. B. Go, M. Eddaoudi, A. J. Matzger, M. O'Keefe, O. M. Yaghi, *Nature* **2004**, *427*, 523–527; g) S. Noro, S. Kitagawa, M. Kondo, K. Seki, *Angew. Chem. Int. Ed.* **2000**, *39*, 2081–2084; h) M. Latroche, S. Surblé, C. Serre, C. Mellot-Draznieks, P. L. Llewellyn, J.-H. Lee, J.-S. Chang, S. H. Jhung, G. Férey, *Angew. Chem. Int. Ed.* **2006**, *45*, 8227–8231; i) S. R. Batten, K. Murray, *Coord. Chem. Rev.* **2003**, *246*, 103–130; j) B. Moulton, J. Lu, R. Hajndl, S. Hariharan, M. J. Zaworotko, *Angew. Chem. Int. Ed.* **2002**, *41*, 2821–2824; k) L.-X. Dai, *Angew. Chem. Int. Ed.* **2004**, *43*, 5726–5729; l) C. Janiak, *Dalton Trans.* **2003**, 2781–2804.

[3] a) G. Bhosekar, I. Jeß, C. Näther, *Inorg. Chem.* **2006**, *43*, 6508–6515; b) C. Näther, I. Jeß, *Inorg. Chem.* **2006**, *45*, 7446–7454; c) C. Näther, I. Jeß, *Inorg. Chem.* **2003**, *42*, 2968–2976; d) C. Näther, I. Jeß, N. Lehnert, D. Hinz-Hübner, *Solid State Sci.* **2003**, *5*, 1343–1357; e) C. Näther, I. Jeß, *J. Solid State Chem.* **2002**, *169*, 103–112; f) C. Näther, J. Greve, *J. Solid State Chem.* **2003**, *176*, 259–265; g) C. Näther, I. Jeß, *Eur. J. Inorg. Chem.* **2004**, 2868–2876; h) C. Näther, M. Wriedt, I. Jeß, *Inorg. Chem.* **2003**, *42*, 2391–2397.

[4] C. Näther, G. Bhosekar, I. Jeß, *Inorg. Chem.* **2007**, in press.

[5] J. Breu, W. Seidl, D. Huttner, F. Kraus, *Chem. Eur. J.* **2002**, *8*, 4454–4460.

[6] J. Pickardt, B. Staub, *Z. Naturforsch.* **1996**, *51b*, 947–951.

[7] G. M. Sheldrick, *SHELXS-97 and SHELXL-97*, University of Göttingen, Germany, **1997**.

[8] *X-Shape, Version 1.03 and X-Red, Version 1.11*, STOE & CIE GmbH, Darmstadt, Germany, **1998**.